# Reports

## Direct Observation of the Femtosecond Excited-State *cis-trans* Isomerization in Bacteriorhodopsin

RICHARD A. MATHIES, C. H. BRITO CRUZ,* WALTER T. POLLARD, CHARLES V. SHANK

**Femtosecond optical measurement techniques have been used to study the primary photoprocesses in the light-driven transmembrane proton pump bacteriorhodopsin. Light-adapted bacteriorhodopsin was excited with a 60-femtosecond pump pulse at 618 nanometers, and the transient absorption spectra from 560 to 710 nanometers were recorded from −50 to 1000 femtoseconds by means of 6-femtosecond probe pulses. By 60 femtoseconds, a broad transient hole appeared in the absorption spectrum whose amplitude remained constant for about 200 femtoseconds. Stimulated emission in the 660- to 710-nanometer region and excited-state absorption in the 560- to 580-nanometer region appeared promptly and then shifted and decayed from 0 to ~150 femtoseconds. These spectral features provide a direct observation of the 13-*trans* to 13-*cis* torsional isomerization of the retinal chromophore on the excited-state potential surface. Absorption due to the primary ground-state photoproduct J appears with a time constant of ~500 femtoseconds.**

FEMTOSECOND OPTICAL MEASUREMENT techniques with a time resolution of ~6 fs (*1, 2*) provide a means of directly observing the temporal evolution of chemical reactions (*3*). These pulses were first used to study energy redistribution among vibronic levels of molecules in solution with a dynamic hole-burning technique (*4*). The primary events in important photobiological systems can also be studied with these techniques. This report describes the use of femtosecond optical absorption to directly observe the excited-state *trans* → *cis* photoisomerization of the retinal prosthetic group within the energy-transducing protein bacteriorhodopsin (BR).

This protein, found in the purple membrane of *Halobacterium halobium*, is responsible for light-driven transmembrane proton pumping (*5*). A variety of experiments have argued that the initial photochemistry involves a 13-*trans* to 13-*cis* isomerization of the bound all-*trans* retinal protonated Schiff base chromophore (*6, 7*) (structure **1**).

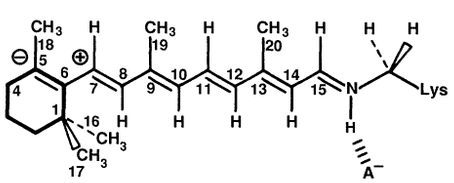


There is considerable interest in determining the molecular mechanism of this photoisomerization. Early picosecond optical studies suggested that the conversion of $BR_{568}$ ($\lambda_{max}$ = 568 nm) to what was then thought to be the primary photoproduct K occurred in 11 ps (*8*). Shortly after this work, Ippen *et al.* (*9*) measured the formation of a photoproduct within 1 ps. Later experiments, using pulses from 120 to 600 fs in duration, demonstrated that a precursor to K (called J) forms in ~500 fs and relaxes to K on a 3-ps time scale (*10–13*).

To temporally resolve the excitation and subsequent photoisomerization of the $BR_{568}$ chromophore it is necessary to study this transformation with 6-fs optical pulses. Because the spectral width of a transform-limited 6-fs pulse is extremely broad (useful measurement range ~3700 $cm^{-1}$), these pulses present the unique opportunity to observe the full spectral response of the system on this rapid time scale. These pulses are also faster than the ground-state recovery time, allowing us to perform dynamic hole-burning experiments to investigate dephasing and energy relaxation. The determination of the dynamics of these processes is especially important because fluorescence quantum yield studies (*14*), theoretical calculations (*15*), and resonance Raman intensity analyses (*16, 17*) have indicated that the time scales for torsional isomerization and excited-state relaxation in rhodopsins are extremely fast.

The experimental apparatus used to perform femtosecond time-resolved spectroscopy on BR is similar to that used for conventional pump-probe experiments except that the probe pulse is approximately 6 fs in duration (*1*) and has a significantly broader bandwidth than the 60-fs pump pulse. The pump and probe pulses are derived from the same amplified 60-fs optical pulse having an energy of 1 μJ and a center wavelength of 618 nm. The 6-fs probe pulse is formed by passing a portion of the initial pulse through a 12-mm length of optical fiber and then through a grating-pair compressor with prism compensation to accurately adjust the time position of the frequency components. The shortened probe pulse then passes through the excited sample to the spectrometer and diode array detector. Care is taken to compensate for group velocity dispersion in the optical path of the probe. The experiments are performed at a repetition rate of 8 kHz.

The light-adapted purple membrane suspension (optical density 0.37 for the 300-μm path length) was pumped through a nozzle at a sufficient velocity to ensure complete replacement of the sample between each pair of laser shots. The data were collected by means of a differential measuring technique. The pump beam was periodically blocked by a shutter at a frequency of 10 Hz, and transmittance spectra were accumulated according to the phase of the chopped pump beam. The time delay for the spectra was determined by an optical delay line controlled by a motor-driven translation stage. The integration time for a single spectrum was typically 30 s.

The differential probe transmittance for pump-probe time delays between −54 and 998 fs includes four distinct contributions (Fig. 1). The dominant feature is the broad hole that forms between 560 and 630 nm and reflects the bleaching of the $BR_{568}$ absorption band. Competing with this at short times, however, are a band of increased transmittance to the red of 650 nm and a strong band of increased absorption to the blue of 580 nm. The former we attribute to stimulated emission from the excited electronic state and the latter to excited-state absorption from $S_1$ to $S_n$ (see Fig. 2). Both features have largely disappeared by 100 to 150 fs, which therefore represents the "relaxation time" of the optically prepared state (*18*). The excited-state absorption band at 580 nm blue-shifts to <560 nm between −28 and 98 fs. Although some of this spectral evolution must be due to its overlap with the growing hole band, the latter is largely complete at 58 fs. A compelling interpretation is that this blue shift results from the excited-state torsional distortion of

R. A. Mathies and W. T. Pollard, Department of Chemistry, University of California, Berkeley, CA 94720.
C. H. Brito Cruz and C. V. Shank, Electronics Research Laboratory, AT&T Bell Laboratories, Holmdel, NJ 07733.

*On leave from Instituto de Fisica, Universidade de Campinas 13100, Campinas, S.P., Brazil.

the retinal chromophore before its radiationless return to the ground state. Finally, the appearance of a red absorption band between 222 and 998 fs results from the formation of the ground-state photoproduct J.

The development of the hole spectrum between 560 and 630 nm deserves further comment. At early times (−54 to −28 fs) the bleach has the width and approximate position of the pump pulse. Later, another sharp feature forms near 590 nm and evolves into the broad, featureless band seen after 58 fs. This short-time behavior, observed in other experiments, has recently been explained as a manifestation of coherent coupling between the pump and probe pulses (*19*). Only after these pulses are temporally separated (≥58 fs) does the observed spectrum reflect the homogeneous line shape (*16*) of the bleached absorption band. Interference from the absorption of the excited state and of the primary photoproduct make it difficult to directly measure the homogeneous line shape in this experiment. A more detailed analysis of the hole spectra based on the theory of (*19*) and the characterization of the $BR_{568}$ $S_1$ state obtained from resonance Raman intensities (*16*) is necessary (*20*).

The data in Fig. 1 reveal the details of the time course of the double-bond isomerization in BR. First, the stimulated emission signal appears promptly and relaxes back to baseline by ~100 fs followed by the appearance of the J absorption from 200 to 1000 fs. The time constant for the appearance of J is ~500 fs, consistent with earlier measurements (*9–13*). The appearance of the J absorption signal and the synchronous filling in of the hole at 568 nm after the loss of the stimulated emission signal argues against the interpretation of J as an excited-state transient (*21*). Furthermore, the 0.5-ps decay of the excited-state absorption (*11*) indicates that the disappearance of the stimulated emission signal is too fast to be due to electronic decay. The rapid attenuation of the stimulated emission signal is best attributed to the ~100-fs torsional distortion of the retinal chromophore on the excited-state potential surface, which shifts the emission to higher wavelengths (Fig. 2). From 100 to 200 fs no emission signal is seen, suggesting that the chromophore has relaxed to a "90° twisted" geometry in the excited state, which has weak radiative coupling with the ground-state surface in the spectral region observed.

The 580 → <560 nm blue shift of the excited-state absorption features from −28 to 98 fs is also consistent with the idea that this is the time scale for excited-state torsional relaxation. As the chromophore distorts on the photochemically active surface, excited-state absorption to torsionally flatter surfaces will shift to the blue. This is entirely consistent with the observation of a strong excited-state absorption band at 460 nm in the 0.5-ps spectrum of Sharkov *et al.* (*11*). The amplitude of the bleach, as indicated by the depth of the hole at ~580 nm, is nearly constant from 28 to 220 fs, whereas the stimulated emission and excited-state absorption signals evolve strongly from 0 to 150 fs. This supports the idea that the optical excitation is largely complete by the 28-fs spectrum and that the temporal evolution of the spectra from 28 to 150 fs provides a direct observation of the excited-state photoisomerization process in BR.

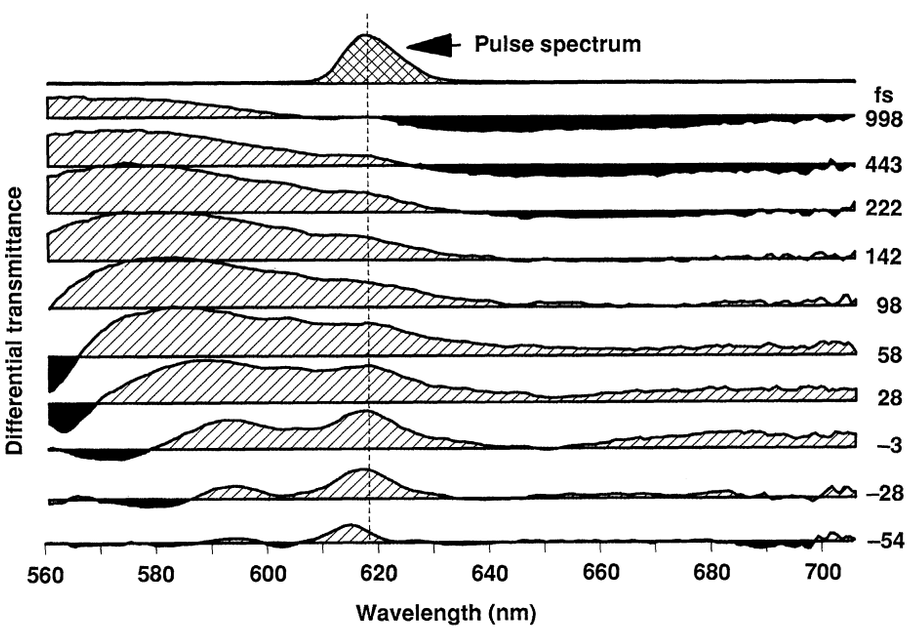


**Fig. 1.** Transient absorption spectra of light-adapted bacteriorhodopsin ($BR_{568}$) at different delay times. The pump pulse at 618 nm (dashed line) had a duration of 60 fs, and the delayed probe pulses were 6 fs in duration. The pump pulse produced a bleach of ~1%, and the signals were linear to a tenfold reduction in either the pump or the probe power.

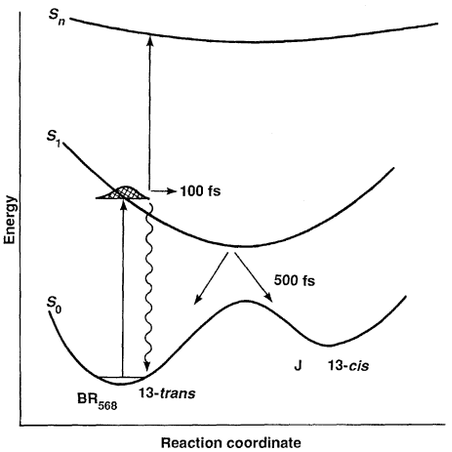


**Fig. 2.** Schematic ground- and excited-state potential surfaces for the double bond 13-*trans* → 13-*cis* isomerization in BR. The vertical arrows indicate the initial absorption, stimulated emission, and excited-state to excited-state absorption processes.

The broad hole (~1000 $cm^{-1}$) observed in the $BR_{568}$ absorption at times ≥28 fs supports the interpretation of the excited-state optical properties of rhodopsins derived from resonance Raman intensities (*16, 17*) and provides a means for the direct connection between time-domain and frequency-domain analyses of the homogeneous line shape in $BR_{568}$. The electronic excitation in $BR_{568}$ produces very large changes in the geometry of the retinal chromophore that drive it rapidly and permanently away from the Franck-Condon geometry. This gives rise to a homogeneous line shape built up from extensive Franck-Condon progressions in multiple modes, each of which has a broad intrinsic homogeneous line width (*16, 17*). We believe that this line width is due to "vibronic dephasing" caused by large changes in both the electronic and the vibrational properties as the chromophore torsionally distorts. The molecule is excited to an essentially dissociative potential surface and, after a rapid initial distortion, experiences dephasing and strong radiationless coupling to the ground state, which prevent it from returning to the Franck-Condon region. The absence of oscillations in the stimulated emission signal indicates the critically damped nature of the torsional isomerization.

*Note added in proof*: This work was first reported at the Second European Conference on the Spectroscopy of Biological Molecules, Freiburg, Federal Republic of Germany, 6 to 10 September 1987. Also, recent experiments on BR with 120-fs time resolu-

tion support the interpretation of the dynamics presented here (*22*).


REFERENCES AND NOTES

1. R. L. Fork *et al.*, *Opt. Lett.* **12**, 483 (1987).
2. C. V. Shank, *Science* **233**, 1276 (1986).
3. For example, the photochemical dissociation of ICN has recently been probed with 100-fs optical pulses [M. Dantus, M. J. Rosker, A. H. Zewail, *J. Chem. Phys.* **87**, 2395 (1987)].
4. C. H. Brito Cruz *et al.*, *Chem. Phys. Lett.* **132**, 341 (1986).
5. W. Stoeckenius and R. A. Bogomolni, *Annu. Rev. Biochem.* **51**, 587 (1982).
6. S. O. Smith, J. Lugtenburg, R. A. Mathies, *J. Membrane Biol.* **85**, 95 (1985).
7. R. R. Birge, *Annu. Rev. Biophys. Bioeng.* **10**, 315 (1981).
8. M. L. Applebury *et al.*, *Biophysics J.* **23**, 375 (1978).
9. E. P. Ippen *et al.*, *Science* **200**, 1279 (1978).
10. M. C. Nuss *et al.*, *Chem. Phys. Lett.* **117**, 1 (1985).
11. A. V. Sharkov, A. V. Pakulev, S. V. Chekalin, Y. A. Matveetz, *Biochim. Biophys. Acta* **808**, 94 (1985).
12. H.-J. Polland *et al.*, *Biophys. J.* **49**, 651 (1986).
13. J. W. Petrich *et al.*, *Chem. Phys. Lett.* **137**, 369 (1987).
14. A. G. Doukas *et al.*, *Proc. Natl. Acad. Sci. U.S.A.* **81**, 4790 (1984).
15. R. R. Birge and L. M. Hubbard, *J. Am. Chem. Soc.* **102**, 2195 (1980).
16. A. B. Myers *et al.*, *J. Chem. Phys.* **79**, 603 (1983).
17. G. R. Loppnow and R. A. Mathies, *Biophys. J.*, in press.
18. Because of the spectral evolution during the first 150 fs, it is questionable to extract simple first-order kinetic constants for the early processes with the absorbance data at just a single wavelength.
19. C. H. Brito Cruz *et al.*, *IEEE J. Quantum Elect.* **24**, 261 (1988).
20. W. T. Pollard *et al.*, in preparation.
21. R. R. Birge, L. A. Findsen, B. M. Pierce, *J. Am. Chem. Soc.* **109**, 5041 (1987).
22. J. Dobler *et al.*, *Chem. Phys. Lett.*, in press.


23. Supported by NIH grant GM 27057 and NSF grant CHE 86-15093.

12 January 1988; accepted 8 March 1988


# The Nature of the Interior of Uranus Based on Studies of Planetary Ices at High Dynamic Pressure


W. J. NELLIS, D. C. HAMILTON, N. C. HOLMES, H. B. RADOUSKY, F. H. REE, A. C. MITCHELL, M. NICOL



**Data from the Voyager II spacecraft showed that Uranus has a large magnetic field with geometry similar to an offset tilted dipole. To interpret the origin of the magnetic field, measurements were made of electrical conductivity and equation-of-state data of the planetary "ices" ammonia, methane, and "synthetic Uranus" at shock pressures and temperatures up to 75 gigapascals and 5000 K. These pressures and temperatures correspond to conditions at the depths at which the surface magnetic field is generated. Above 40 gigapascals the conductivities of synthetic Uranus, water, and ammonia plateau at about 20 (ohm-cm)$^{-1}$, providing an upper limit for the electrical conductivity used in kinematic or dynamo calculations. The nature of materials at the extreme conditions in the interior is discussed.**


THE VOYAGER II SPACECRAFT DATA showed that Uranus has a strong magnetic field, which can be described approximately by a dipole of moment 0.23 G $R_U^3$, where $R_U$ is the planetary radius (25,600 km). The dipole is centered at 0.3 $R_U$ and its axis is tilted 60° from the axis of rotation. The maximum value at the surface is 1.1 G (*1*), twice the value for Earth, and the minimum surface value is 0.1 G. These unexpected and unusual Voyager data emphasize the need for laboratory measurements of planetary materials at interior conditions in order to derive planetary models consistent with the observational data. We report new shock-wave electrical conductivity and equation-of-state (EOS) data for planetary "ices" and for a liquid with an atomic composition representative of a mixture of the "ices." Our electrical conductivity data provide density and temperature dependences up to 75 GPa (0.75 Mbar) and 5000 K and provide an upper bound that can be used in kinematic and dynamo calculations to explain the magnetic field. Laboratory data and theory also allow us to hypothesize on the nature of the interior.

The composition of Uranus is estimated from the mass, radius, rotational rate, and gravitational field (*2, 3*). The combined magnetic-field and radio-emission data yielded an improved measurement of the rotation rate of 17.24 hours (*4*). This result led to improved values of the density moments, which are derived from the gravitational moments deduced from the observed precessions of the elliptical rings of Uranus. The density moments provide a constraint on the equations of state of candidate materials. Prior to Voyager II, Hubbard and MacFarlane proposed that Uranus consists of three layers: an outer gas layer of $H_2$-He; a middle "ice" layer composed mostly of $H_2O$, $CH_4$, and $NH_3$; and an inner rocky core (*2*). The "ices" are actually in the fluid phase over a substantial portion of these proposed thermodynamic conditions.

After Voyager II, Kirk and Stevenson proposed that the magnetic field and the density moments derived from improved values of the rotation rate and gravitational moments are consistent with a greater degree of material mixing (*5*) than in the pre-Voyager models. One model consists of an outer gas-ice-rock region, which is mostly an $H_2O$-$H_2$ mixture, and an inner rocky core. The boundary is at 0.3 $R_U$ and 300 GPa and 6000 K. The magnetic field is produced primarily in an $H_2O$-rich region near 0.7 $R_U$ at 50 to 100 GPa, based on a kinematic model that considers equatorial zonal jet flow and uses the electrical conductivity of water extrapolated from Holzapfel's (*6*) fit to static and shock data up to 10 GPa and 1300 K. The Voyager II data were used by Gudkova *et al.* (*7*) and they also found more mixing. Their three-layer model has an outer $H_2$-He-ice region, a middle ice-rock layer, and an inner rocky core. The outer-middle boundary at 0.71 $R_U$ is at 30 GPa and 2700 K and the middle-core boundary at 0.14 $R_U$ is at 600 GPa and 6800 K. Their two-layer model is ice-rock for radii less than 0.72 $R_U$ at 25 GPa and 2600 K, with $H_2$-He-rock-ice being the remainder. The vari-

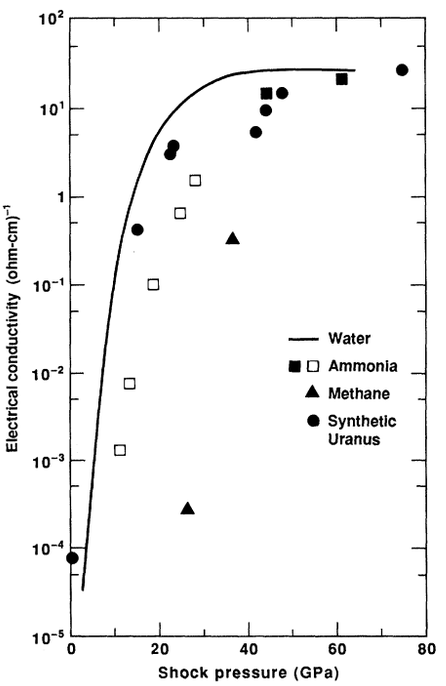


**Fig. 1.** Electrical conductivity versus shock pressure for planetary fluids. Solid symbols are the present work. Open squares are from (*16*). Solid curve is smooth curve through the data of (*9*) and (*12*). At 40 GPa, temperatures in these fluids are 2600 K in water, 2800 K in synthetic Uranus, 3100 K in ammonia, and 4100 K in methane.


W. J. Nellis, Physics Department and Institute of Geophysics and Planetary Physics, University of California, Lawrence Livermore National Laboratory, Livermore, CA 94550.
D. C. Hamilton, N. C. Holmes, H. B. Radousky, F. H. Ree, A. C. Mitchell, Physics Department, University of California, Lawrence Livermore National Laboratory, Livermore, CA 94550.
M. Nicol, Department of Chemistry and Biochemistry, University of California, Los Angeles, CA 90024.